

A multiscale approach for the study of x-ray radiation effects in paediatric patients subjected to interventional cardiology procedures

Maria Souli^{1,2}, Agapi Ploussi^{1,3}, Ellas Spyratou^{1,3}, Ioannis Seimenis¹

¹Medical Physics Laboratory, School of Medicine, Democritus University of Thrace, Alexandroupolis, Greece

²Physics Department, School of Applied Mathematical and Physical Sciences, National Technical University of Athens, Athens, Greece

³2nd Department of Radiology, Medical Physics Unit, National and Kapodistrian University of Athens, Attikon University Hospital, Athens, Greece

SUBMISSION: 30/12/2019 - ACCEPTANCE: 5/3/2020

ABSTRACT

Purpose: Paediatric dosimetry requires a patient-specific approach due to the long-life expectancy and high radiosensitivity of children. The main aim of the current study was to study physical and biological dosimetric characteristics, as well as the effect of x-ray radiation on the biochemical properties of lymphocytes in paediatric patients who underwent interventional cardiology (IC) procedures.

Material and Methods: A total of 10 paediatric patients who underwent IC procedures with a biplane angiographic system was enrolled in the study. Physical dosimetry was performed by converting dose-area-product

to effective dose with the use of appropriate k-factors taking into account patient's body size. Peripheral blood samples were collected from each patient before and immediately after the IC procedure. Biodosimetry, for the detection of radiation-induced DNA damage, was based on the assessment of the protein biomarker γ -H2AX. Furthermore, biomechanical properties of unirradiated and irradiated lymphocytes were evaluated using atomic force spectroscopy.

Results: Effective doses (EDs) estimated for the studied cases ranged from 0.6 to 16.7 mSv. Immunofluorescence microscopy detected a small increase in γ -H2AX



CORRESPONDING
AUTHOR,
GUARANTOR

Agapi Ploussi,
Medical Physics Laboratory, School of Medicine, Democritus University of Thrace, Alexandroupolis, Greece-2nd Department of Radiology, Medical Physics Unit, National and Kapodistrian University of Athens, Attikon University Hospital, 12462, Athens, Greece, Email: aplousi@gmail.com

foci formation in post-exposure blood samples even in EDs lower than 10 mSv. A decrease in elasticity was observed in lymphocytes of the irradiated blood samples. The Young's modulus was increased from 1-8 KPa in un-irradiated lymphocytes to 1.8-11 KPa in irradiated ones.

Conclusions: This work applied a multiscale method-

ology to explore the radiogenic effects, even down at subcellular level, from diagnostic x-rays in paediatric IC. Exposure of peripheral blood lymphocytes to low dose ionising radiation seems to increase DNA damage and cellular stiffness, although correlation with ED was not observed.



KEY WORDS

Paediatric dosimetry; γ -H2AX; Biodosimetry; Elastic modulus; Atomic force spectroscopy; Interventional cardiology

1. Introduction

The number of interventional radiology and interventional cardiology (IC) procedures performed has increased significantly over the last two decades [1]. Concerning paediatric population, a study conducted by International Atomic Energy Agency (IAEA) showed that paediatric interventional procedures occupy a significant portion of the adult procedure's workload in many countries [2]. Studying paediatric exposure to ionising radiation requires special considerations: children are at higher risk of developing radiation-induced cancers compared to adults due to their longer life expectancy and their rapidly dividing cells, they have a wide variation in body size and radiation-induced cancer risk is strongly dependent on age. In addition, paediatric patients with congenital diseases are often subjected to repeated examinations employing ionising radiation over their lifetime, thus absorbing significant cumulative doses [3]. Therefore, paediatric dosimetry must be patient-specific, considering not only the exposure parameters but also the patient's somatometric and biological characteristics.

Low-level ionising radiation exposure from diagnostic and therapeutic devices is monitored by using sensitive physical or chemical dosimeters that can detect doses between 0.1 and 50 mGy at a reference position. This position however is outside of the body and, thus, such measurements cannot accurately represent the dose deposited in the human body. This underlines the need for performing parallel biodosimetry to acquire information about the dose absorbed by the organism and the actual biological effects. Towards this direction, many ideas and methods have been developed, one of which focus-

es on the DNA damage induction in the cell nucleus: the major radiation absorber and target. Ionising radiation exposure may induce Double Strand Breaks (DSBs), Single Strand Breaks (SSBs), base damage (oxidation or loss) or a combination of the above in clustered types of DNA lesions [4], with the type and extent of damage depending on radiation characteristics and complexity level. DSBs are the most important lesions and their impaired repair is strongly correlated with radiosensitivity [5]. After a DSB induction and during the early steps of cellular response, the repair pathway involves the activation of proteins that sense and control DNA damage. Among these proteins is H2AX, a variant form of the histone H2A that undergoes phosphorylation at DSB sites and creates γ -H2AX clusters observed as distinct foci under a fluorescence microscope. γ -H2AX formation is proportional to dose, peaks at ~30 min post-exposure and declines over time [6]. A strong correlation between DSBs and γ -H2AX foci has been reported [7].

Beyond chemical and biophysical processes, leukocytes also perform mechanical functions. The biomechanical properties of leukocyte cytoskeleton (stiffness, adhesion, elasticity) are correlated with immune modulation mechanics such as migration, adhesiveness to the endothelium and deformability through the capillaries [8, 9]. The degree of the effective mechanical repair and mechanical properties restoration plays a critical role to the pathology of many disorders [10, 11]. However, only a few studies have been referred to the characterisation of the leukocyte nano-mechanical changes in relation to disease diagnosis and/or prognosis. Changes in cell deformability can be assessed through various methods [12-14]. Among them, atomic force microscopy (AFM)

is a powerful nanotool which can combine cell imaging and measurement of mechanical properties. AFM is a scanning probe microscopy technique that creates three-dimensional micrographs with resolution down to the nanometer and Angstrom scales, by utilising a nano-tip (probe) attached to a flexible cantilever of a specific spring constant. It records the amount of force felt by the cantilever as the probe tip is brought close to -and even indented into- a sample surface and then pulled away [15]. Thus, AFM can elucidate local mechanical properties in living cells [16, 17] and detect relevant changes induced by ionising radiation [15].

The aim of the current study was to investigate the effect of x-ray radiation, at cellular and subcellular levels, in paediatric patients who underwent IC procedures. To this scope, DNA breaks and biomechanical properties were evaluated in peripheral blood lymphocytes prior to and after x-ray exposure, while the findings were benchmarked against estimated effective doses.

2. Material and Methods

The study was approved by the Research and Ethics Committee of the Institution where the IC procedures were performed. Written informed consent was obtained from all parents/guardians.

2.1. Patient cohort and exposure conditions

A cohort of 10 paediatric patients with congenital heart diseases, who underwent diagnostic and/or therapeutic IC procedures for various heart defects including atrial septal defect (n=3), tetralogy of Fallot (n=2), patent ductus arteriosus (n=2), pulmonary artery stenosis (n=2) and coarctation of the aorta (n=1), were enrolled in the study. Patient demographic and somatometric data (gender, age, weight and height) were recorded for all patients. Study inclusion criteria included patient age (≤ 16 years), fluoroscopy time (≥ 2.5 min) and number of acquisitions (≥ 4), whilst exclusion criteria included comorbid disease (potentially affecting leukocyte condition) and participation of a second cardiologist in the procedure performed. All IC procedures were performed by the same experienced cardiologist using a biplane angiographic system (Artis Zee, Siemens Healthcare) equipped with a flat panel detector and automatic exposure technique (AEC). The system used had an inherent filter of 2.5 mm Al and additional copper filters ranging from 0.1 to 0.9 mm Cu. The available fields of view (FOV) were 10, 16, 20

and 25 cm. Exposure parameters including tube voltage, fluoroscopy time, cine runs, number of frames and total dose area product (DAP) per projection angle were collected from the corresponding dose reports. Total DAP represents the cumulative DAP for both fluoroscopy and cine angiography.

2.2. Physical dosimetry and estimation of effective dose

Effective dose (ED) was derived from total DAP using appropriate DAP-to-effective dose conversion factors. Conversion factors were adopted by Schmidt et al. [18], who determined them for different projection angles by using Monte Carlo techniques and mathematical body phantoms representing children aged 0, 1, 5, 10 and 15 years. In the current study, imaging was performed in only two projection angles (anteroposterior-AP and lateral-LAT). Therefore, ED was estimated for each patient as follows in equation 1:

$$ED = \left(k_{age}^{AP} \times \frac{BW_{ph}}{BW} \times f_{kVp}^{AP} \times f_{filt}^{AP} \times DAP^{AP} \right) + \left(k_{age}^{LAT} \times \frac{BW_{ph}}{BW} \times f_{kVp}^{LAT} \times f_{filt}^{LAT} \times DAP^{LAT} \right) \quad (\text{equation 1})$$

where k_{age}^{AP} and k_{age}^{LAT} are the age-adjusted DAP-to-effective dose conversion factors for the AP and LAT exposures, respectively

BW_{ph} and BW are the body weights of the phantom and the patient, respectively

f_{kVp}^{AP} and f_{kVp}^{LAT} are the tube voltage correction factors for the AP and LAT exposures, respectively

f_{filt}^{AP} and f_{filt}^{LAT} are the beam filtration correction factors for the AP and LAT exposures, respectively

DAP^{AP} and DAP^{LAT} are the total dose area product for the AP and LAT exposures, respectively.

2.3. Detection of DNA damage by immunofluorescence

Peripheral blood from each study participant was collected before (to serve as control) and right after the IC procedure. The blood samples consisted of circulating blood obtained from the catheter, so no additional venipuncture was necessary. Lymphocytes were isolated from each sample, distended in KCl solution and attached on slides (via Cytospin sample chamber). Subsequently, indirect immunofluorescence assay was performed, including (main steps) cells permeabilisation, blocking of non-specific binding, immunostaining with primary γ -H2AX antibody (rabbit, IF 1:1000, Cat: NB100-79967, Novus Biologicals, Abingdon, UK) and secondary

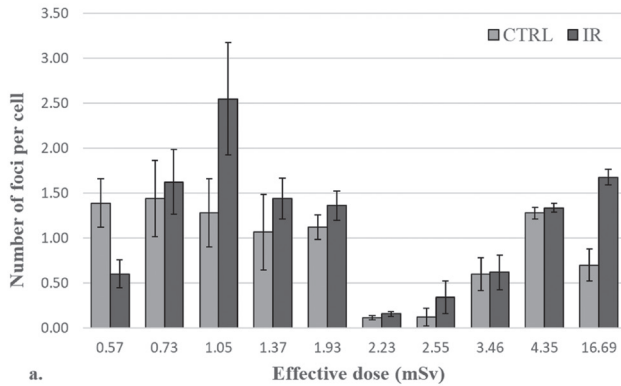
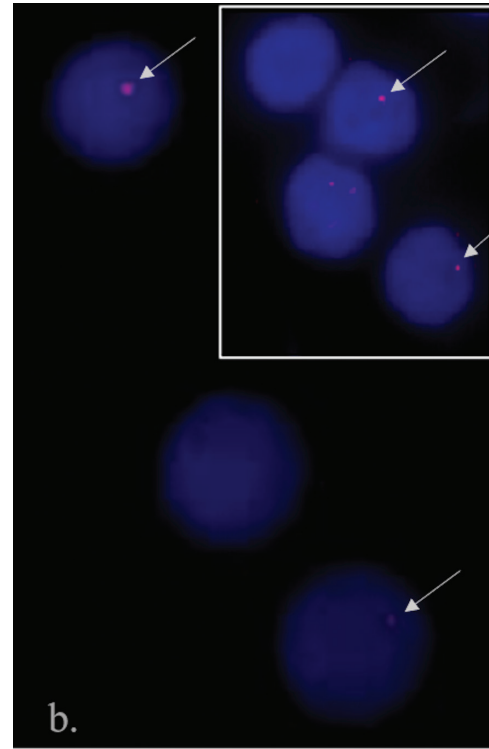


Fig. 1. a. Mean number of DSB foci per cell in corresponding control (CTRL) and irradiated (IR) samples vs the effective dose estimated for each exposure. Error bars indicate standard error of the mean. **b.** Representative images of lymphocytes stained for γ -H2AX detection. Red, γ -H2AX foci; blue, nucleus stained with DAPI. Arrows indicate foci that were taken into account. Cells under stress are easily distinguishable among background cells.



fluorescent antibody (Rhodamine Red-X anti-rabbit, IF 1:4000, Cat: R6394, Life Technologies) and final nuclear stain with DAPI. Analysis was performed under a fluorescent microscope (AxioPlan 2, Carl Zeiss Microscopy GmbH, Hamburg, Germany), using the Isis imaging software (Metasystems, Altlußheim, Germany). The number of foci in 200-300 nuclei were measured for each sample collected.

2.4. Assessment of the elastic modulus by atomic force microscopy

During the lymphocyte isolation procedure, 1 ml of cells in culture medium (from each sample) was transferred on glass coverslips contained in petri dishes, incubated for 1 hour and fixed. The elastic modulus of the irradiated lymphocytes was measured in relation to that of the non-irradiated lymphocytes by using AFM (Nanoscope diInnova, Veeco metrology, Santa Barbara CA) with an Innova scanner possessing a maximum range of 100 X 100 X 7.6 μm . Silicon nitride cantilevers were calibrated by the thermal tune method [19] and provided a spring constant of $k=0.01$ N/m. AFM tips were imaged independently utilising scanning electron microscopy (SEM) and an average radius value of 40 nm was obtained.

Atomic force topography of the lymphocytes was recorded by using the contact mode of AFM. In contact mode, also known as repulsive mode, the tip is constantly in close contact to the sample surface, resulting in soft “physical contact” during the scanning process. Force-distance curves were produced by recording the lymphocyte pushback on the tip (deflection) versus vertical z position of the tip probe. Analysis was performed using selected force curves in Spmlab analysis software ver. 7.0.0.1 (Veeco, Malvern PA). The slope in the linear region of the force curve represents the sample stiffness. For each sample collected, 50 force curves were recorded. To obtain quantitative differences in the elasticity of the lymphocytes, the tip indentation dz into the soft sample was calculated as the difference of the respective Z positions relative to the ideal hard (glass) surface. The applied force is given by equation 2 as a function of the indentation depth of the AFM tip, according to the Hertz-Sneddon model [20]:

$$F = \frac{4}{3} \frac{E \sqrt{R}}{(1-\nu^2)} dz^{3/2} \quad (\text{equation 2})$$

where F is the loading force, E is the Young’s modulus, ν is the Poisson ratio, R is the radius of the AFM tip and dz is the indentation of the AFM tip into the lymphocyte.

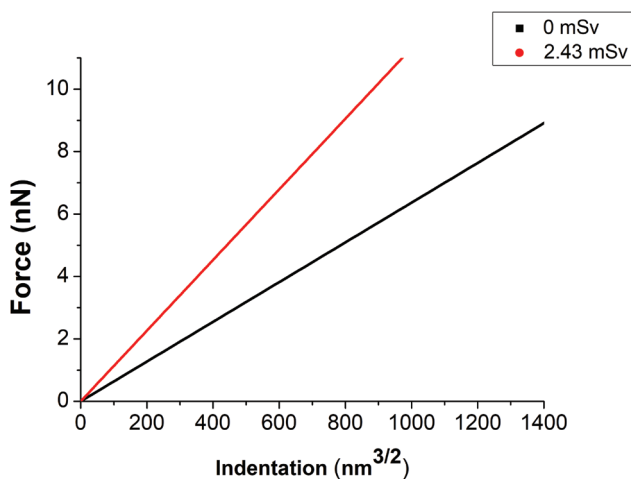


Fig. 2. Force curves for an unirradiated lymphocyte (corresponding to 0 mSv) and an irradiated lymphocyte (corresponding to a cardiac catheterisation with 2.43 mSv effective dose).

Thus, the Young's modulus was calculated from the slope of the linear curve, which fits the plot of force versus indentation^{3/2}, according to the equation 3:

$$E = \frac{3(1-\nu^2)}{4\sqrt{R}} \frac{dF}{dz^{3/2}} \quad (\text{equation 3})$$

Cells membranes are generally assumed to be quasi incompressible, characterised by a Poisson ratio of 0.50. A tip radius of 40 nm and a cantilever spring constant of 0.01 N/m were used in all calculations.

3. Results

Patient demographic and somatometric data, along with the main exposure parameters, are summarised in **Table 1**. Additional copper filtration ranged from 0.1 to 0.6 mm Cu, but for the estimation of ED the correction factor corresponding to 0.1 mm Cu was used (since correction factors for thicker Cu filtration are not provided in [18]). All the available FOVs were used depending on the IC procedure and the child's age, but since there was no recording of FOV, a corresponding correction factor was not applied. Mean ED (\pm standard deviation) was found, according to equation 1, equal to 3.64 ± 5.06 mSv (ranging from 0.57 to 16.69 mSv). Estimated effective dose per subject included in the study is shown in **Fig. 1a**.

Fig. 1. depicts the excess DNA damage to peripheral blood lymphocytes potentially caused by the low dose exposure during the IC procedure performance. **Fig. 1a**,

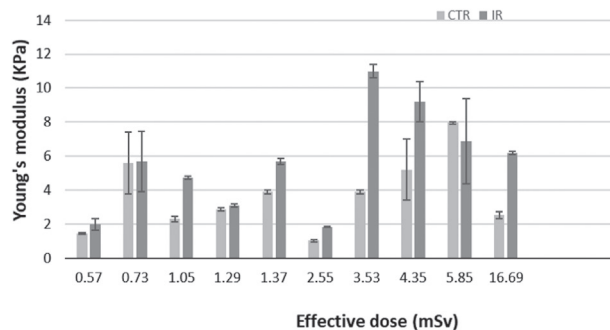


Fig. 3. Mean elastic moduli, measured for unirradiated (CTRL) and irradiated (IR) lymphocytes, vs estimated effective dose for each study participant. Error bars indicate standard error of the mean.

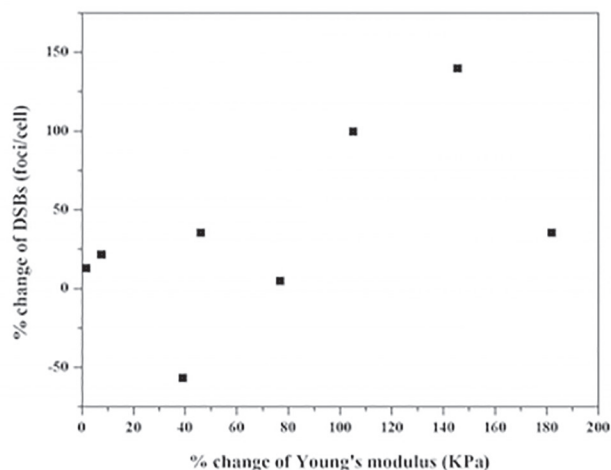


Fig. 4. Percentage change of the mean number of DSBs per cell (γ -H2AX foci per cell) vs the percentage change of the mean elastic modulus.

which illustrates the average number of detected DSB foci per cell, suggests a tendency for a small increase in the number of foci in irradiated samples compared to the corresponding control (unirradiated) ones. Only for the subject with the lowest effective dose estimated (0.57 mSv), foci identified in the unirradiated sample outnumbered those found in the respective irradiated one. To acquire the mean values presented in **Fig. 1a**, more than 200 cells per sample were evaluated for foci identification. As seen in **Fig. 1b**, foci of different sizes and intensities were formed, from which only the largest, most contrasted against their background and most well-de-

Table 1. Patient characteristics and exposure parameters expressed in Mean \pm standard deviation

Table 1. Patient characteristics and exposure parameters expressed in Mean \pm standard deviation	
Patient characteristics	
Age (years)	6.29 \pm 5.30 [0.25-16]
Gender	7 Females/3 Males
BW (kg)	25.18 \pm 20.08 [4.6-60]
BMI (kg/m ²)	17.15 \pm 3.28 [13.38-23.42]
Exposure parameters	
Tube Voltage (kVp)	70.4 \pm 7.2 [57-97]
Fluoroscopy time (min)	6.80 \pm 3.32 [2.80-12.60]
Number of acquisitions (cine runs)	12.11 \pm 6.39 [4-24]
Number of frames	1010 \pm 781 [328-2580]
Total DAP (μ Gy*m ²)	1185.01 \pm 2091.86 [36.35-6528.9]

BW: Body weight; BMI: Body Mass Index; Values in brackets indicate range

finer ones were taken into account. Unlike *ex vivo* blood irradiations with relatively high doses [6] that cause the formation of several large, sharp and bright foci in every cell (since all cells within the sample volume are irradiated), *in vivo* low dose irradiations, such as that described herein, induce a few small, unsharpened and mild foci in a cell portion only of the blood sampled.

Atomic force topography did not reveal any morphological changes of the lymphocytes for the dose range studied. **Fig. 2** shows representative force curves (i.e. loading force vs tip indentation) corresponding to unirradiated lymphocytes and irradiated lymphocytes collected from the study participant receiving an effective dose of 2.43 mSv. **Fig. 3** illustrates the change in the measured Young's modulus potentially associated with the exposure of children to x-rays during cardiac catheterisation. The comparison between mean moduli values obtained from unirradiated and irradiated samples suggests that low dose irradiation may increase cellular stiffness. It is obvious, however, that this increase is variable and not correlated to the estimated effective dose.

Fig. 4 shows the percentage change of the mean number of DSBs (γ -H2AX foci per cell) against the percentage change of the mean elastic modulus for the same estimated effective doses.

4. Discussion

A better knowledge of patient x-ray dose and the associated radiation risk in paediatric patients is imperative

in view of the extensive use of x-rays and the higher radiosensitivity of children. This is particularly important for patients with congenital heart diseases, who are often subjected to repeated IC procedures associated with high radiation doses. Therefore, dosimetry in paediatric patients undergoing IC procedures would greatly benefit from a patient-specific approach. The main goal of the current study was to propose and implement a hybrid methodology aiming at providing relevant information mainly at cellular but also at organismal level. More specifically, aspects of physical and biological dosimetry were combined with cellular biomechanical properties to evaluate, on an individualised basis, radiogenic effects in paediatric cardiac catheterisation.

Expression of γ -H2AX is commonly used to estimate DNA damage and, therefore, γ -H2AX focus yield constitutes a useful quantitative biomarker for individuals that are exposed to ionising radiation. Moreover, lymphocytes are considered to be a good reference target due to their high radiosensitivity in comparison to the other types of peripheral blood cells [21], whilst venous blood can be easily sampled. Biodosimetry data of this study indicate that low dose irradiations, such as those involved in the IC procedures studied, may slightly increase the γ -H2AX foci levels identified in peripheral blood lymphocytes sampled from paediatric patients. Current findings are consistent with those reported in a previous *in vivo* study which also involved paediatric patients subjected to

cardiac catheterisations with a median effective dose of 6.4 mSv [22]. Although the number of radiation-induced foci was variable, a small increase in γ -H2AX foci number was demonstrated for the vast majority of the study participants after irradiation. Nevertheless, current results shown in **Fig. 1a** suggest that at such low doses, the dose response of the radiation-induced γ -H2AX foci (DSBs) *in vivo* is not linear. This finding, also reported in [22], could be partly attributed to the high inter-subject variability, mainly due to differences in radiosensitivity and repair capacity. On the other hand, the small number of participants in this study and the limited accuracy in estimating ED and γ -H2AX foci per cell have also played a contributing role.

Other researchers found an 8-10-fold increase in γ -H2AX foci of blood samples taken 5 minutes after chest-abdominal-pelvic computed tomography, with the yield though corresponding to a mean radiation dose of 16.4 mGy delivered at a relatively high dose rate [23]. In another study, it was demonstrated that partial body exposures, simulated by mixing *ex vivo* irradiated and unirradiated lymphocytes, γ -H2AX foci distributions were significantly over-dispersed compared to uniformly irradiated lymphocytes [24]. Going one step further, it has been suggested that using γ -H2AX detection to determine the extent of DSB induction may help to identify precancerous cells, to stage cancers, to monitor the effectiveness of cancer therapies and to develop novel anticancer drugs [25]. It is hypothesised, therefore, that immunostaining datasets like the present one may help achieve personalised estimation of the radiogenic risks associated with medical procedures utilising x-rays, and may also provide useful insight into determining overall cell health.

Acquired AFM results indicate that the exposure of paediatric patients to low dose x-ray radiation may affect the biomechanical properties of the membrane cytoskeleton of lymphocytes. As documented in the literature, the values of Young's modulus for human healthy lymphocytes lie in the range of 0.41-1.4 KPa [26, 27]. In the studied cohort of paediatric patients, Young's modulus of unirradiated lymphocytes ranged from 1 to 8 KPa, whilst lymphocytes collected after exposure revealed a range from 1.8 to 11 KPa. It is hypothesised, therefore, that ionising radiation not only may inflict biological effects on lymphocytes but can also influence the mechanical properties of their membrane cytoskeleton. No

correlation was seen between estimated ED and change in Young's modulus, partly due to the small study cohort and the limited accuracy in ED estimation and in the measurement of elastic modulus. Similarly, no correlation was found between the change in elastic modulus and the number of DBS foci per cell. However, focused work is required to investigate potential associations between the biological processes that take place into the cells during exposure to x-rays and the irradiation-induced changes in their mechanical behaviour.

The small size of the patient cohort studied constitutes the major limitation of the current study. A small number of subjects were recruited mainly due to the fact that only a portion of patients subjected to IC procedures met the inclusion criteria designated. One additional limitation lies in the ED estimation. As known, DAP-to-effective dose conversion factors depend on several factors including patient's body size, tube voltage, beam filtering, projection angle and field size. In the current study, field size was not considered. Moreover, the employed DAP-to-effective dose conversion factors are based on prior data from ICRP Publication 60, while they have been determined for an image-intensifier fluoroscopy system and not a flat panel one. The relatively high variation in the age at irradiation among subjects studied and in the employed exposure parameters are further confounding factors. The age at irradiation of paediatric patients critically affects radiosensitivity and even small age differences may result in significantly varying biological effects for the same irradiation, while different exposure conditions may have variable impact on the same subject.

In conclusion, this study combined DSB and cellular stiffness measurements in peripheral blood lymphocytes acquired from a paediatric population subjected to IC procedures. It is postulated that the observed increase in DNA damage and in cellular stiffness does not correlate with the effective dose associated with the exposure. Undoubtedly, further research is warranted to fully investigate the potential association between radiation-induced DNA damage and radiation-induced changes in the biomechanical properties of lymphocytes, as well as to fully couple these subcellular effects to the radiogenic risk as expressed by the effective dose. **R**

Conflict of interest

The authors declared no conflicts of interest.

Acknowledgments:

1. This research is co-financed by Greece and the European Union (European Social Fund-ESF) through the Operational Programme "Human Resources Development, Education and Lifelong Learning 2014-2020" under the call for proposals "Supporting researchers with emphasis on new researchers" (EDULLL 34), in the context of the project "Patient-specific dosimetry for paediatric patients under-

going interventional cardiology procedures" (82089-MIS 5006356).

2. The authors would like to thank Dr Spyridon Rammos, Director of Paediatric Cardiology and Adult with Congenital Heart Disease Department, Onassis Cardiac Surgery Center, Athens, Greece for providing them access to the clinical data. Thanks are also due to Prof. Alexandros Georgakilas and Dr Georgia Terzou-di for their advice on the γ H2AX technique.

REFERENCES

1. Hart D, Wall BF, Hiller MC, et al. Frequency and collective dose for medical and dental X-ray examinations in the UK, 2008. *Health Protection Agency* 2010, HPA-CRCE-012.
2. Tsapaki V, Ahmed N, AlSuwaidi JS, et al. Radiation exposure to patients during IR procedures in 20 countries. Initial IAEA project results. *AJR Am J Roentgenol* 2009; 193(2): 559-569.
3. Ait-Ali L, Andreassi MG, Foffa I, et al. Cumulative patient effective dose and acute radiation-induced chromosomal DNA damage in children with congenital heart disease. *Heart* 2010; 96(4): 269-274.
4. Nikitaki Z, Vladimir, N, Mavragani IV, et al. Non-DSB clustered DNA lesions. Does theory colocalize with the experiment? *Rad Phys Chem* 2016; 128: 26-35.
5. Löbrich M, Shibata A, Beucher A, et al. γ H2AX foci analysis for monitoring DNA double-strand break repair: Strengths, limitations and optimization. *Cell Cycle* 2010; 9(4): 662-669.
6. Redon CE, Dickey JS, Bonner WM, et al. γ -H2AX as a biomarker of DNA damage induced by ionizing radiation in human peripheral blood lymphocytes and artificial skin. *Adv Space Res* 2009; 43(8): 1171-1178.
7. Rogakou EP, Pilch DR, Orr AH, et al. DNA double-stranded breaks induce histone H2AX phosphorylation on serine 139. *J Biol Chem* 1998; 273(10): 5858-5868.
8. Dragovich MA, Genemaras K, Dailey HL, et al. Dual regulation of L-Selectin-mediated leukocyte adhesion by endothelial surface glycocalyx. *Cell Mol Bieng* 2017; 10: 102-113.
9. Vicente-Manzanares M, Sánchez-Madrid F. Role of the cytoskeleton during leukocyte responses. *Immunology* 2004; 4: 110-122.
10. Alexandrova A, Antonova N. Rheological and mechanical aspects of leukocytes motion and adhesion. *Series on Biomechanics* 2012; 27: 74-79.
11. Wautier JL, Schmid-Schonbein GW, Nash GB, et al. Measurement of leukocyte rheology in vascular disease: clinical rationale and methodology. *Clin Hemorheol Microcirc* 1999; 21: 7-24.
12. Evans EA. Bending elastic modulus of red blood cell membrane derived from buckling instability in micropipette aspiration tests. *Biophys J* 1983; 43: 27-30.
13. Bransky A, Korin N, Nemirovski Y, et al. An automated cell analysis sensing system based on a microfabricated rheoscope for the study of red blood cells physiology. *Biosens Bioelectron* 2006; 22: 165-169.
14. Li Y, Wenb C, Xiea H, Ye A, et al. Mechanical property analysis of stored red blood cell using optical tweezers. *Colloids Surf B Biointerfaces* 2009; 70: 169-173.
15. Spyratou E, Dilvoi M, Patatoukas G, et al. Probing the effects of ionizing radiation on Young's modulus of human erythrocytes cytoskeleton using atomic force microscopy. *J Med Phys* 2019; (2): 113-117.
16. Cappella B, Dietler G. Force-distance curves by

- atomic force microscopy. *Surf Sci Rep* 1999; 34: 1-104.
17. Thomas G, Burnham NA, Camesano TA, et al. Measuring the mechanical properties of living cells using atomic force microscopy. *J Vis Exp* 2013; 76: e50497.
 18. Schmidt PWE, Dance DR, Skinner CL, et al. Conversion factors for the estimation of effective dose in paediatric cardiac angiography. *Phys Med Biol* 2000; 45: 3095-3107.
 19. Hutter JL, Bechhoefer J. Calibration of atomic-force microscope tips. *Rev Sci Instrum* 1993; 64: 1868-1873.
 20. Sneddon IN. The relation between load and penetration in the axisymmetric Boussinesq problem for a punch of arbitrary profile. *Int J Eng Sci* 1965; 3: 47-56.
 21. Heylmann, D, Rodel F, Kindler T, et al. Radiation sensitivity of human and murine peripheral blood lymphocytes, stem and progenitor cells. *Biochim Biophys Acta* 2014; 1846(1): 121-129.
 22. Beels L, Bacher K, De Wolf D, et al. gamma-H2AX foci as a biomarker for patient X-ray exposure in paediatric cardiac catheterization: are we underestimating radiation risks? *Circulation* 2009; 120(19): 1903-1909.
 23. Rothkamm K, Balroop S, Shekhdar J, et al. Leukocyte DNA damage after multi-detector row CT: a quantitative biomarker of low-level radiation exposure. *Radiology* 2007; 242(1): 244-251.
 24. Horn S, Barnard S, Rothkamm K. Gamma-H2AX-based dose estimation for whole and partial body radiation exposure. *PLoS One* 2011; 6(9): e25113.
 25. Bonner WM, Redon CE, Dickey JS, et al. γ H2AX and cancer. *Nat Rev Cancer* 2008; 8(12): 957-967.
 26. Cai X, Cai J, Dong S, et al. Morphology and mechanical properties of normal lymphocyte and Jurkat revealed by atomic force microscopy. [Article in Chinese]. *Sheng Wu Gong Cheng Xue Bao* 2009; 25: 1107-1112.
 27. Kuznetsova TG, Starodubtseva MN, Yegorenkov NI, et al. Atomic force microscopy probing of cell elasticity. *Micron* 2007; 38: 824-883.



READY-MADE
CITATION

Souli M, Ploussi A, Spyratou E, Seimenis I. A multiscale approach for the study of x-ray radiation effects in paediatric patients subjected to interventional cardiology procedures. *Hell J Radiol* 2020; 5(1): 19-27.